Scintillating fiber detectors for time evolution measurement of the triton burnup on the Large Helical Device

Scintillating fiber detectors for time evolution measurement of the triton burnup on the Large Helical Device[a)]

Neng Pu,[1 b)] Takeo Nishitani,[2] Kunihiro Ogawa,[1,2] Hiroki Kawase,[1] Mitsutaka Isobe,[1,2] and LHD Experiment Group[1]

[1]*SOKENDAI (The Graduate University for Advanced Studies), 322-6 Oroshi-cho, Toki 509-5292, Japan*
[2]*National Institute for Fusion Science, National Institutes of Natural Sciences, 322-6 Oroshi-cho, Toki 509-5292, Japan*

(Presented XXXXX; received XXXXX; accepted XXXXX; published online XXXXX)
Two scintillating fiber (Sci-Fi) detectors have been operated in the first deuterium plasma campaign of the Large Helical Device (LHD) in order to investigate the time evolution of the triton burnup through secondary 14 MeV neutron measurement. Two detectors use scintillating fibers of 1 mm diameter embedded in an aluminum matrix with a length of 10 cm connect to the magnetic field resistant photomultiplier. A detector with 91 fibers was developed in Los Alamos National Laboratory and has been employed on JT-60U. Another detector with 109 fibers has been developed in National Institute for Fusion Science. The signals are fed into a discriminator of 300 MHz bandwidth with pulse counter module for on-line measurement and a digitizer of 1 GHz sampling with 14 bits to acquire pulse shape information for off-line data analysis. The triton burnup ratio has been evaluated shot-by-shot by the 14 MeV neutron measurement of Sci-Fi detectors which are calibrated by the neutron activation system and the total neutron measurement of the neutron flux monitor using ^{235}U fission chambers. The time evolution of triton burnup is investigated in different plasma configurations on LHD.

I. INTRODUCTION

The Large Helical Device (LHD) is a large superconducting heliotron device in Japan, having a major radius of 3.9 m and averaged plasma minor radius of ~0.6 m.[1] In the LHD, the deuterium plasma operation started in March 2017 to explore high-performance deuterium plasmas of LHD. There are two reactions to produce 2.45 MeV neutrons and 1 MeV tritons in deuterium plasmas. The production rate of 2.45 MeV neutrons and 1 MeV tritons are almost the same. Energetic tritons will undergo secondary D-T reaction with background deuteron while those tritons slow down. Kinematic properties such as the Larmor radius and the precessional drift frequency of 1 MeV tritons are almost the same as those of 3.5 MeV alphas in D-T plasmas. Therefore, the triton burnup study is useful to estimate the behavior of D-T born alphas in deuterium plasmas. To evaluate the absolute neutron yield from LHD deuterium plasmas, a wide dynamic range neutron flux monitor (NFM)[2] and a neutron activation system (NAS)[3] are employed in LHD.[4] The NFM on LHD consists of three ^{235}U fission chambers and three high-sensitivity thermal neutron detectors. The NFM plays a primary role in the evaluation of the total neutron yield. Although NAS does not provide time evolution of neutron emission rate, it is absolutely insensitive to gamma-rays and is of great value for performing cross check of the neutron yield evaluated by NFM.[5,6] In the tokamaks such as TFTR[7], JET[8], ASDEX-U[9], JT-60U[10], DIII-D[11], FT[12], PLT[13], and KSTAR[14], neutron activation techniques have been applied to measure the shot integral primary 2.45 MeV neutron yields and secondary 14 MeV neutron yields in the deuterium plasmas. The scintillating fiber (Sci-Fi) detector has been developed by the Los Alamos National Laboratory (LANL) and was utilized for the time-resolved 14 MeV neutron measurement on TFTR[15] and JT-60U[16]. The Sci-Fi detector has a high counting rate capability (higher than 10^7 counts/s) and good discrimination characteristic for 2.45 MeV neutrons and gamma-rays, consequently, is suitable for the time-resolved triton burnup measurement.

In the first deuterium campaign of LHD, two Sci-Fi detectors work for time evolution of 14 MeV neutron measurement. Two detectors use scintillating fibers of 1 mm diameter embedded in an aluminum (Al) matrix with length of 10 cm, which connect to the magnetic field resistant photomultiplier tube (PMT) for signal output. A detector with 91 fibers was developed in LANL, which is named LANL Sci-Fi detector. Another detector with 109 fibers has been developed in National Institute for Fusion Science (NIFS), which is named NIFS Sci-Fi detector. A new compact NIFS Sci-Fi detector and data acquisition system (DAQ) are described in section II. Calibration of two Sci-Fi detectors by NAS measurement is shown in section III. Time evolutions of triton burnup 14 MeV neutron emission rate on LHD are given in section IV. Finally, the operation of Sci-Fi detectors in this campaign is summarized in section V.

II. EXPERIMENTAL SETUP

Figure 1 (a) and 1 (b) show the picture of the LANL Sci-Fi detector and the NIFS Sci-Fi detector. The NIFS Sci-Fi

[a)]Published as part of the Proceedings of the 22nd Topical Conference on High-Temperature Plasma Diagnostics (HTPD 2018) in San Diego, California, USA.
[b)] Author to whom correspondence: pu.neng@nifs.ac.jp

detector is a newly developed compact detector consisting of 109 fibers as a diameter of 1 mm and a length of 10 cm. The fibers were embedded into aluminum matrix for stopping recoil proton and electron passing into adjacent fiber to reduce the contribution from low-energy neutrons and gamma-rays as shown in Fig. 1(c). The acryl plate of 10 mm thickness is a light guide for fiber and is an insulation layer for an aluminum matrix and a PMT window. A PMT assembly H6152-70 of magnetic registrant is used for signal output. The total length of the detector is less than 22 cm. This compact Sci-Fi detector will be helpful for the development of a 14 MeV neutron camera.

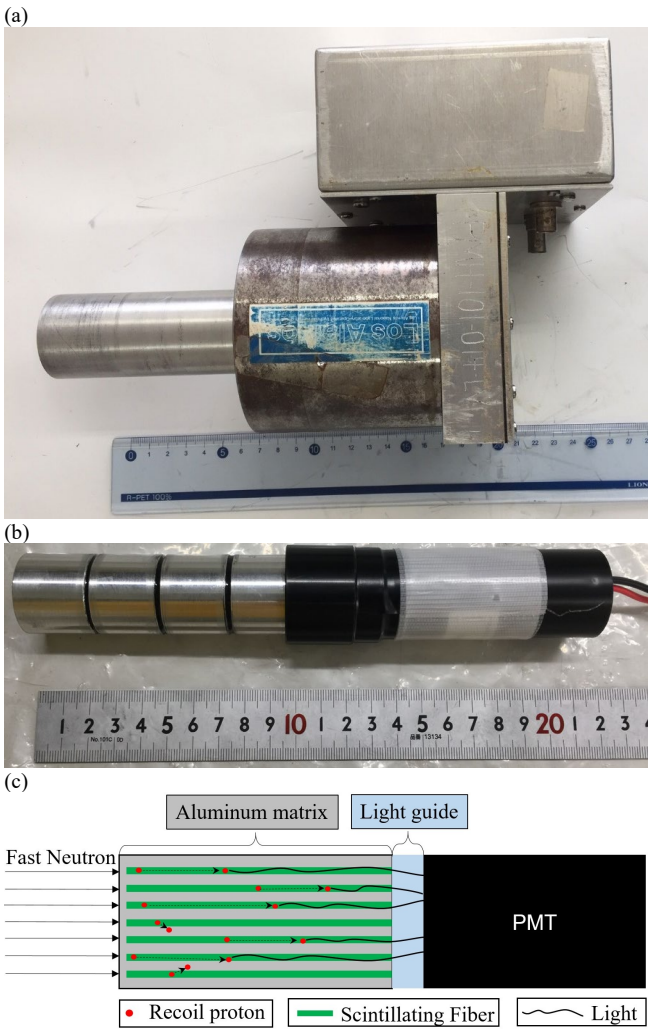

FIG. 1. (a) Overview of LANL Sci-Fi detector with 91 fibers of 1 mm diameter and a length of 10 cm, (b) overview of NIFS Sci-Fi detector with 109 fibers of 1 mm diameter and a length of 10 cm, (c) the principle of Sci-Fi detector: the signal is induced by the energy of protons or electrons deposited in fibers; in other words, the signal can not be produced when the protons or electrons runaway form the fiber and is absorbed by Al matrix. Note that, light guide is not used for the LANL Sci-Fi detector. The plastic matrix was applied to connect the Al head of LANL Sci-Fi detector and PMT window.

The setup of detectors is shown in Fig. 2. The LANL Sci-Fi detector is located on the outside of 8-O port, and the NIFS Sci-Fi detector is located on the outside of 2.5-L port. The distance from the two detectors to plasma center is around 4 m. The block diagram of electronics and DAQ is also shown in Fig. 2. In the LHD experiment, the ORTEC 556 was used as a high voltage direct current power supply for Sci-Fi detectors. The anode signals of PMT are divided into two signals, which is directly fed into the DAQ and the NIM module in the basement by coaxial cables of 10 m and 20 m with input impedance of 50 ohms for each detector as shown in Fig. 2. The NIM module is employed for on-line measurement with fixed threshold, which consists of a FAN-IN/FAN-OUT module to change negative pulse to positive pulse, a discriminator of 300 MHz bandwidth and a pulse counter. The DAQ (model NO. APV8102-14MWPSAGb) consists of a digitizer of 1 GHz sampling, analog-to-digital converter (ADC) and the field programmable gate array (FPGA) module for signal processing and data storage. The shaping information of each pulse was stored by 64 sampling points of 1 ns when FPGA received a trigger pulse. Here, pulse width of two Sci-Fi detectors is 10 to 20 ns. The raw data (the shaping information of each pulse) has been used for off-line analysis. Pulse height spectrum and time evolution of integral counts can be obtained.

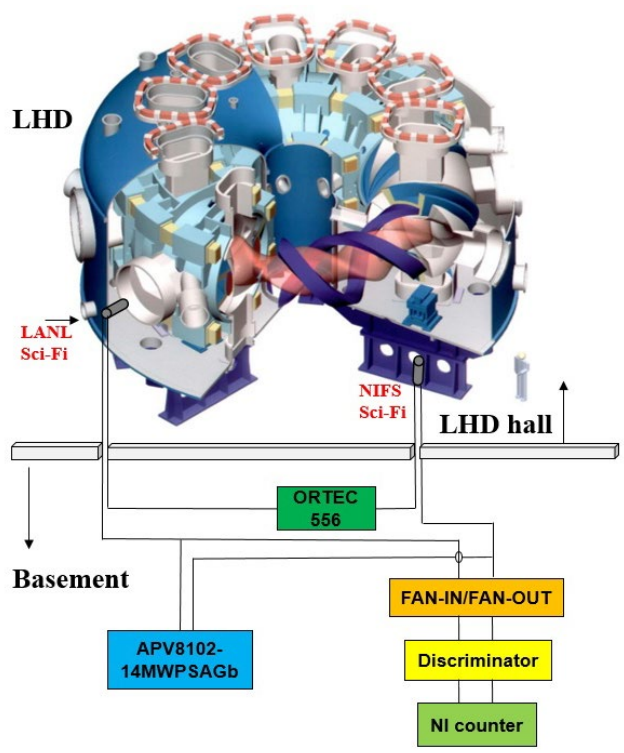

FIG. 2. Experimental setup of Sci-Fi detectors and the block diagram of electronics and data acquisition system.

III. CALIBRATION OF SCI-FI DETECTORS BY NAS MEASUREMENT

The pulse height spectra of two Sci-Fi detectors have shown same characteristic (two decay) in high neutron yield shot and low neutron yield shot as shown in Fig. 3, respectively. In high neutron yield shot (shot No. 141170), the total neutron yield reaches to 2.1×10^{15} n/shot, where line-averaged electron density is 1.5×10^{19} m^{-3}, and the central electron temperature is about 4 keV. In low neutron yield

shot (shot No. 141167), the total neutron yield is 3.9×10^{14} n/shot, where line-averaged electron density is 3×10^{18} m^{-3}, the central electron temperature ranges from 2 to 3 keV. First decay of both spectra in low pulse height region corresponds to the detector signal induced by 2.45 MeV neutrons and gamma-rays. Second decay in higher pulse height region corresponds to the signal induced by 14 MeV neutrons.

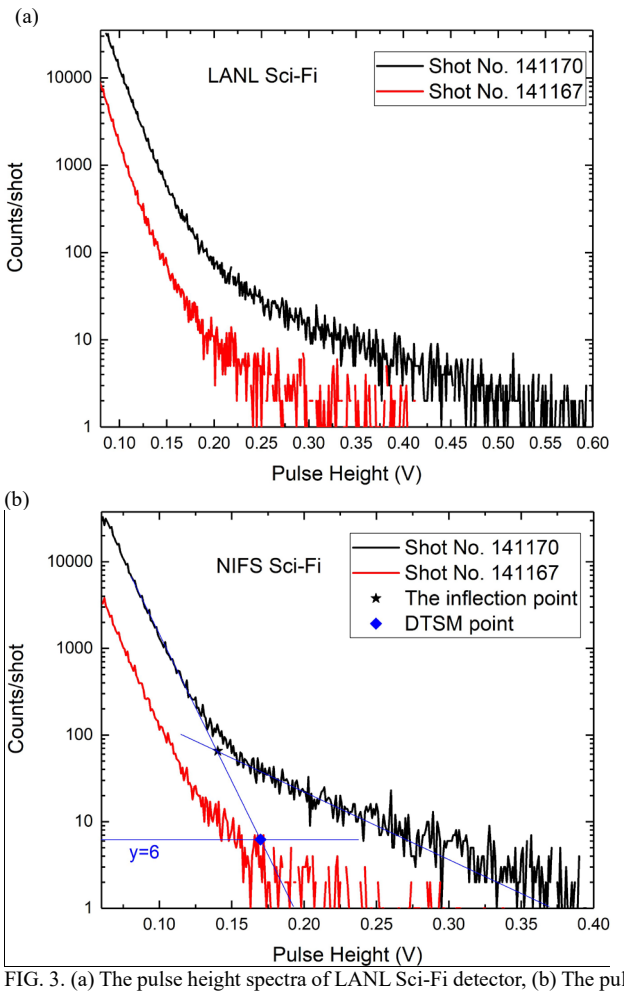

FIG. 3. (a) The pulse height spectra of LANL Sci-Fi detector, (b) The pulse height spectra of NIFS Sci-Fi detector with DTSM for maximum selection of 14 MeV neutron counts without 2.45 MeV neutron counts.

Here, dynamic threshold selection method (DTSM) is defined for maximum selection of 14 MeV neutron counts without 2.45 MeV neutron counts. The DTSM uses the extension cord of first decay with intercept of dynamic selection line (DSL) to fix threshold level for different shots. Here, DSL is defined as y=0.1×(the inflection point y value of two decays). For example, in the pulse height spectra of the NIFS Sci-Fi detector, 130 mV can be a suitable threshold for shot No. 141167, and 170 mV can be a suitable threshold for shot No. 141170. The total neutron yield is high in shot No. 141170. If 130 mV is still chosen for shot No. 141170, the time evolution measurement will include the part from 2.45 MeV neutrons and gamma-rays. As shown in Fig. 3 (b), the inflection point y value of two decays is 61, the DSL is chosen as y=6 for NIFS Sci-Fi detector in shot No. 141170. Pulse counts from 2.45 MeV neutrons and gamma-rays can be negligible when 170 mV can be chosen for the threshold in this shot.

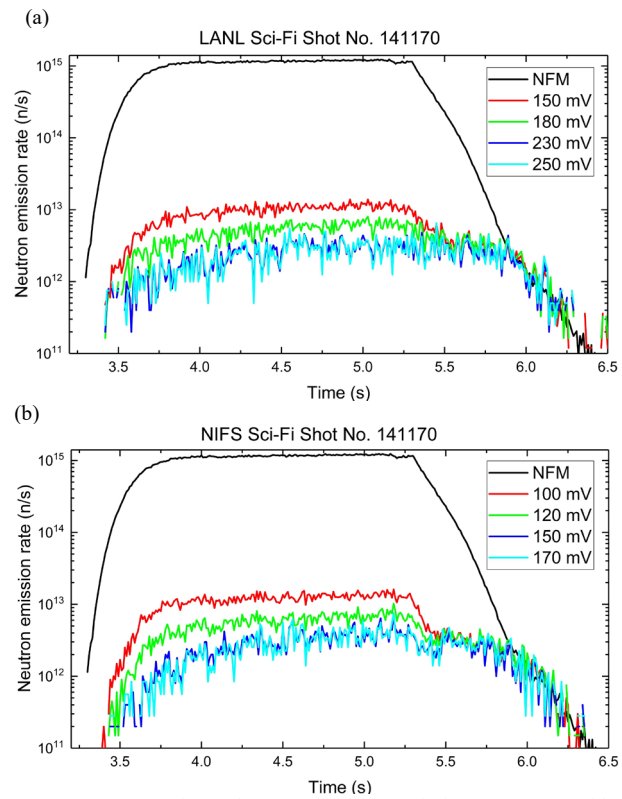

FIG. 4. (a) Comparison of 14 MeV neutron emission rate measured by the LANL Sci-Fi detector with different threshold and total neutron emission rate measured by NFM, (b) Comparison of 14 MeV neutron emission rate measured by the NIFS Sci-Fi detector with different threshold and total neutron emission rate measured by NFM.

In Fig. 4, two Sci-Fi detectors have shown the same time evolution of 14 MeV neutrons with high threshold level and the same influence by 2.45 MeV neutrons with low threshold level in the same shot. In addition to this, time evolution measurements of 14 MeV neutron have shown the same tendency in two different high-threshold case of each Sci-Fi detector, which means that the measurement of Sci-Fi detectors are not effected by 2.45 MeV neutron and gamma-rays in high-threshold case.

Shot-integrated 14 MeV neutrons measured by Sci-Fi detectors have been calibrated by absolute 14 MeV neutron measurement of NAS as shown in Fig. 5. The NIFS Sci-Fi detector shows good linearity with threshold of 170 mV. Due to the neutron flux at the detector position of a horizontal port being higher than that of a low vertical port, calibration of LANL Sci-Fi detector in high neutron yield shots are effected by 2.45 MeV neutrons in the case of the threshold of 250 mV. By using the DTSM, linearity is improved in the calibration of LANL Sci-Fi detector as shown in Fig. 4(a). The triton burnup ratio can be evaluated shot-by-shot by the shot integrated 14 MeV neutron yield measurement of Sci-Fi detectors which calibrated by absolute 14 MeV neutron measurement of NAS and the total neutron measurement of NFM.

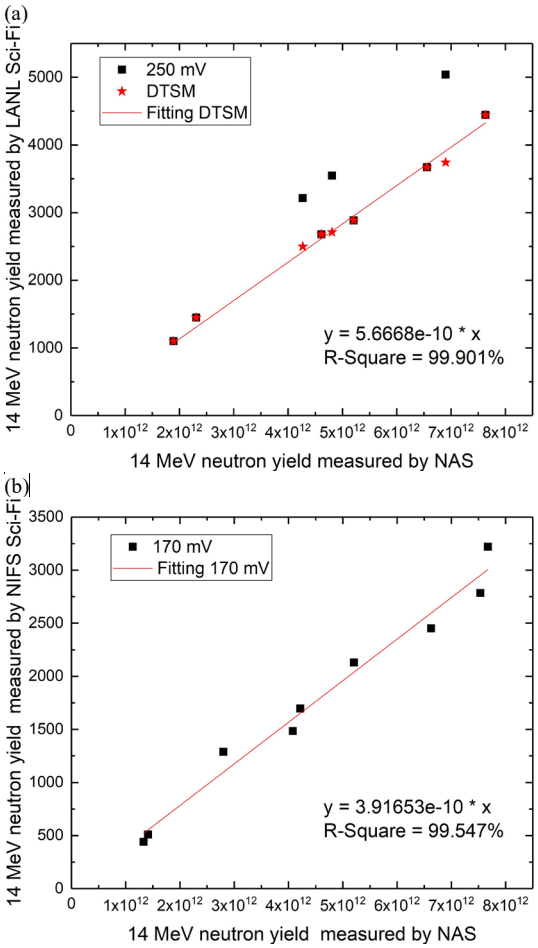

FIG. 5. (a) Shot-integrated 14 MeV neutron pulse counts measured with LANL Sci-Fi detector as a function of 14 MeV neutron yield measured with calibrated NAS, (b) Shot-integrated 14 MeV neutron pulse counts measured with NIFS Sci-Fi detectors as a function of 14 MeV neutron yield measured with calibrated NAS.

VI. TIME EVOLUTION OF TRITON BURNUP ON LHD

Figure 6 shows the time evolutions of secondary 14 MeV neutron emission rate measured with the LANL Sci-Fi detector in the deuterium plasma of different electron densities and different central electron temperature with NBI heating and ECRH heating. The time constant of the building up and the decay of the 14 MeV neutron emission rate measured by the LANL Sci-Fi detector is much longer than those of the total neutron emission rate measured by NFM. 1 MeV triton needs a long time to slow down to energy where cross section (around 170 keV) for secondary D-T reaction is large. In the part of flat density and flat total neutron emission rate of three shots, the rise of 14 MeV neutron emission rate changes to flatter with the decrease of slowing-down time, and the falling of 14 MeV neutron emission rate change to steeper with the decrease of slowing-down time after NBI is turned off, where the slowing-down time is evaluated to be 0.7 s for shot No. 140859, 0.4 s for shot No. 140848, and 0.09 s for shot No. 140415 as shown in Fig. 6 (a), Fig. 6 (b), and Fig. 6 (c), respectively. Triton burnup ratios are evaluated to be 0.29%, 0.34%, and 0.35% in shot No. 140859, shot No. 140848, and shot No. 140415, respectively. This indicates that the confinement property of triton is better in a shorter slowing-down time regime.

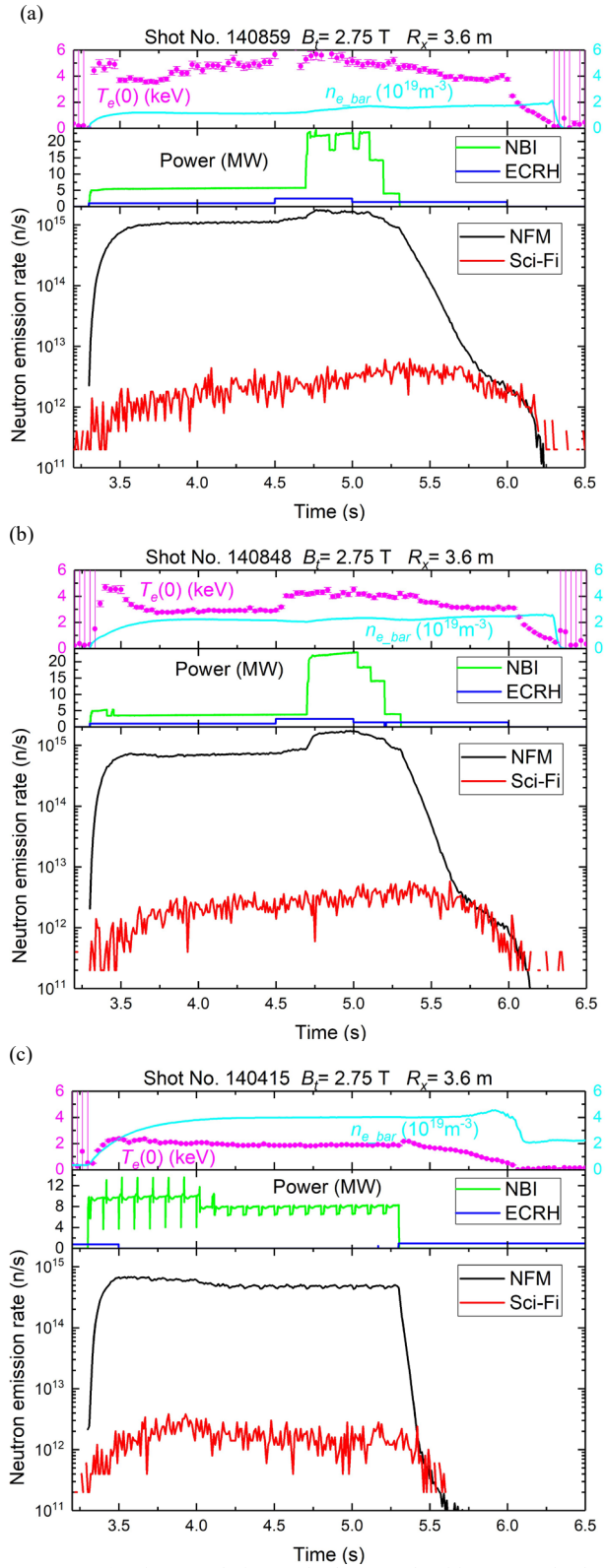

FIG. 6. (a) Time evolutions of electron densities, central electron temperature, NBI power, ECRH power, 14 MeV neutron emission rate measured by the LANL Sci-Fi detector and total neutron emission rate measured by NFM in shot No. 140859, (b) time evolutions of electron densities , central electron temperature, NBI power, ECRH power, 14 MeV

neutron emission rate measured by the LANL Sci-Fi detector and total neutron emission rate measured by NFM in shot No. 140848, (c) time evolutions of electron densities, central electron temperature, NBI power, ECRH power, 14 MeV neutron emission rate measured by the LANL Sci-Fi detector and total neutron emission rate measured by NFM in shot No. 140415.

V. SUMMARY

In the first deuterium campaign of LHD, two Sci-Fi detectors successfully worked to measure time evolution of 14 MeV neutron emission rate for triton burnup study. By using fast digitizer, the shaping information of each pulse was obtained for the off-line analysis on the pulse height spectrum and the time evolution of 14 MeV neutron. By using the digitizer data, threshold for time evolution of 14 MeV neutron can be easily chosen, which is not achieved by using traditional NIM discriminator. This great advantage is helpful for remote threshold setting in control room during the experiment due to that a mass of material will be activated by high neutron yield experiment in the experimental hall and the time of working in hall is restricted by radiation control rule. Also, the suitable threshold was set by comparison of different thresholds, which can exclude the influence from 2.45 MeV neutrons and gamma-rays by using DTSM. By the calibration of shot integrated 14 MeV neutron yield measured by Sci-Fi detectors with absolute 14 MeV neutron measurement of NAS, the triton burnup ratio has been evaluated shot-by-shot. In addition to this, the compact design for the NIFS Sci-Fi detector will be helpful for development of 14 MeV neutron camera in the future.

ACKNOWLEDGMENTS

This work was supported by the LHD project budgets (ULHH003 and ULHH034).

[1] A. Iiyoshi *et al.*, Nucl. Fusion **39** 1245 (1999).
[2] M. Isobe *et al.*, Rev. Sci. Instrum, **85** 11E114 (2014).
[3] N. Pu *et al*., Rev. Sci. Instrum, **88** 113302 (2017).
[4] M. Isobe *et al*., Rev. Sci. Instrum. **81** 10D310 (2010).
[5] L. C. Johnson *et al*., Rev. Sci. Instrum, **66** 894 (1995).
[6] Cris W. Barnes *et al*., Rev. Sci. Instrum, **61** 3190 (1990).
[7] C. W. Barnes *et al*., Nucl. Fusion **38** 597 (1998).
[8] S. Conroy, *et al*, Nucl. Fusion **28** 2127 (1988).
[9] M. Hoek *et al*., IPP-Report IPP-1/320 (1999).
[10] M. Hoek *et al*., Nucl. Instrum. Meth. Phys. Res., A **368** 804 (1996).
[11] H. H. Duong, W. W. Heidbrink, Nucl. Fusion **33** 211 (1993).
[12] P. Batistoni *et al*., Nucl. Fusion **27** 1040 (1987).
[13] W. W. Heidbrink, R. E. Chrien, J. D. Strachan, Nucl. Fusion **23** 917 (1983).
[14] J. Jo *et al*., Rev. Sci. Instrum, **87** 11D828 (2016).
[15] G. A. Wurden *et al*., Rev. Sci. Instrum. **66 (1)** 901 (1995).
[16] T. Nishitani *et al*., Plasma Phys. Control. Fusion **38** 355 (1996).